Politechnika Warszawska

Wydział ...

Kierunek: ...

...

Adam Komorowski i Maciej Domagała

Warszawa, czerwiec 2021

Contents

Introduction

Chapter 1

Theory

1.1 Generative Adversarial Networks

1.1.1 Overview

Generative Adversarial Networks (GANs) is a family of neural networks used in generative modelling. They were proposed in 2014 by Ian Goodfellow et al. in [7].
They have various different applications across deep learning fields e.g. generative models can be used as a tool for data augmentation of small datasets. For instance, one can feed some text written in a particular handwriting as input to a generative model to generate more text in the same handwriting. The following are results of the first facial images generation experiments with GANs. Another use case is generation of super-resolution images, which allows to produce more detailed and high quality version of input images.

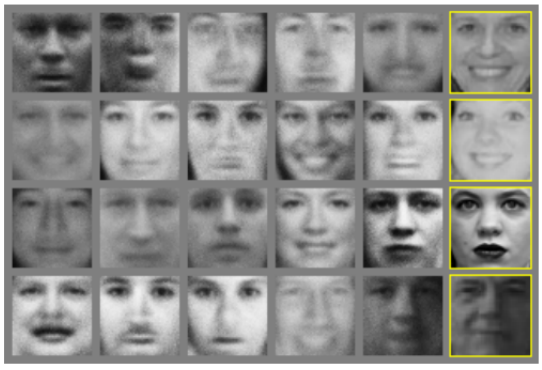

Figure 1.1: Images generated by GAN [7].

Since first examples, GANs networks became an object of intense development, which resulted in increasing quality of generated objects each year.

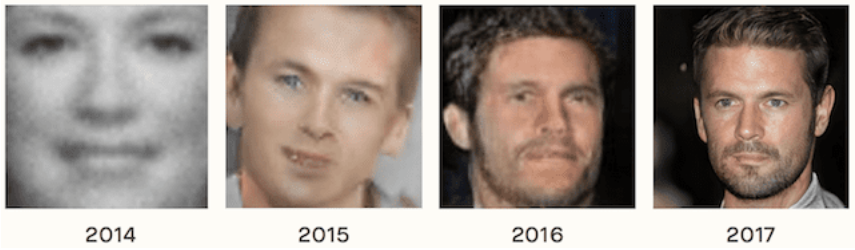

Figure 1.2: Example of progression in the capabilities of GANs [8].

1.1.2 Architecture

Generative adversarial networks are composed of two neural networks, one called the **generator** (denoted as G in this work) and the other called the **discriminator** (denoted as D).
The role of the generator is to estimate the probability distribution of the real samples in order to provide generated samples resembling real data. The discriminator is trained to estimate the probability that a given sample came from the real data rather than being provided by the generator. These structures are called generative adversarial networks because the generator and discriminator are trained to compete with each other: the generator tries to get better at fooling the discriminator, while the discriminator tries to get better at identifying generated samples. GAN architecture can be described using schema below.

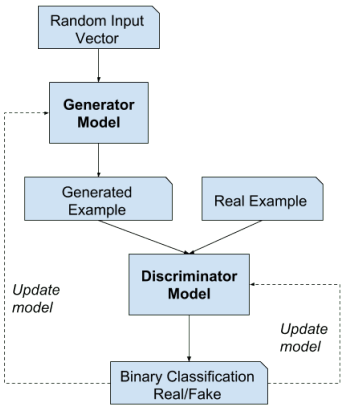

Figure 1.3: GAN architecture [18].

Training

The GAN training process consists of a two-player minimax game. Although the dataset containing the real data isn't labeled, the training processes for discriminator and generator are performed in a supervised way.
For discriminator training, at each iteration we pass some real samples taken from the training data labeled as 1 and some generated samples provided by generator labeled as 0. New images are generated based on noise input derived from e.g. Gaussian distribution. This way, we can use more conventional supervised training frameworks to update the parameters of discriminator. The discriminator outputs a value $D(x)$ indicating the chance that x is a real image. Model objective is to maximize the chance of recognizing real images and generated images as separate classes. To measure the performance the **cross-entropy loss** is used and therefore the objective function can be written as follows:

$$max_D V(D) = \mathbb{E}_{\mathbf{x}\sim p_{data}(\mathbf{x})}[\log D(\mathbf{x})] + \mathbb{E}_{\mathbf{z}\sim p_z(\mathbf{z})}[\log(1 - D(G(\mathbf{z})))]. \tag{1.1}$$

For each batch of training data containing labeled real and generated samples, model updates the parameters of discriminator to optimize the loss function. After the parameters are updated, generator is trained to produce better samples (in terms of quality and variety). The output of generator is connected to discriminator, whose parameters are kept frozen at the time of generator training. On the generator side, it's objective is to generate images with the highest possible value of $D(x)$ to *fool* the discriminator. This condition can be written as:

$$min_G V(G) = \mathbb{E}_{\mathbf{z}\sim p_z(\mathbf{z})}[\log(1 - D(G(\mathbf{z})))]. \tag{1.2}$$

Combining these two aspects, we can define GAN as a minimax game during which generator wants to minimize V function, while discriminator wants to maximize it:

$$min_G max_D V(D, G) = \mathbb{E}_{\mathbf{x}\sim p_{data}(\mathbf{x})}[\log D(\mathbf{x})] + \mathbb{E}_{\mathbf{z}\sim p_z(\mathbf{z})}[\log(1 - D(G(\mathbf{z})))]. \tag{1.3}$$

Once both objective functions are defined, they are learned jointly by the alternat-

ing gradient descent. We fix the generator model's parameters and perform a single iteration of gradient descent on the discriminator using the real and the generated images. Then the roles are switching and the discriminator is fixed while the generator is trained for another single iteration. We train both networks in alternating steps until the generator produces good quality images. The training algorithm for GANs is well summarized in the figure below.

Algorithm 1 Minibatch stochastic gradient descent training of generative adversarial nets. The number of steps to apply to the discriminator, k, is a hyperparameter. We used $k = 1$, the least expensive option, in our experiments.

for number of training iterations **do**

  for k steps **do**

  - Sample minibatch of m noise samples $\{\boldsymbol{z}^{(1)}, \ldots, \boldsymbol{z}^{(m)}\}$ from noise prior $p_g(\boldsymbol{z})$.
  - Sample minibatch of m examples $\{\boldsymbol{x}^{(1)}, \ldots, \boldsymbol{x}^{(m)}\}$ from data generating distribution $p_{\text{data}}(\boldsymbol{x})$.
  - Update the discriminator by ascending its stochastic gradient:

$$\nabla_{\theta_d} \frac{1}{m} \sum_{i=1}^{m} \left[\log D\left(\boldsymbol{x}^{(i)}\right) + \log\left(1 - D\left(G\left(\boldsymbol{z}^{(i)}\right)\right)\right) \right].$$

  end for

  - Sample minibatch of m noise samples $\{\boldsymbol{z}^{(1)}, \ldots, \boldsymbol{z}^{(m)}\}$ from noise prior $p_g(\boldsymbol{z})$.
  - Update the generator by descending its stochastic gradient:

$$\nabla_{\theta_g} \frac{1}{m} \sum_{i=1}^{m} \log\left(1 - D\left(G\left(\boldsymbol{z}^{(i)}\right)\right)\right).$$

end for

The gradient-based updates can use any standard gradient-based learning rule. We used momentum in our experiments.

Figure 1.4: GAN training algorithm pseudocode [7].

It is worth mentioning that a known problem of GAN networks is the fact that not always a smaller value of loss function leads to better results - in practice, a common solution is to empirically evaluate generated results every few iterations, rather than tracking loss. To cope with this problem metrics such as **Inception Score** or **Frechet Inception Distance** were presented.

Inception Score and Fréchet Inception Distance

Inception Score is a metric used especially for measuring the quality of Generative Adversarial Network outputs. It was first proposed in [1] and was used ever since to compare benchmark results of new generative models. Inception Score was defined to measure two important aspects of generative networks performance - quality of

generated images and their diversity. If network produces diverse images of good quality - the score is designed to be high.

Authors used the Inception network [2] to calculate the conditional label distribution for every created image. It is denoted as $p(y|x)$, where y is bounded to label and x is a single image instance. For images of high quality this distribution should have a *low entropy* characteristic - meaning that one class (correct one) should have a high probability score, while the rest should have relatively small scores. This indicates that Inception classifier has a lot of certainty what is presented on given image. To measure diversity, authors proposed to calculate the marginal distribution of y by combining label distributions for a large set of images (50 000 is a proposed value). More formally, if z is a latent vector and $G(z)$ is an image generated from the vector, then marginal distribution

$$p(y) = \int_z p(y \mid x = G(z)) \ dz \tag{1.4}$$

should have *high entropy* (should be close to the uniform distribution) if model has a strong diversifying power.

Combining two above conditions, we can observe that best performing model would have different distributions of $p(y|x)$ and $p(y)$. To link these two discrete distributions together authors decided to use a Kullback-Leibler Divergence formula:

$$D_{KL}(p\|q) = \sum_{i=1}^{N} p\left(x_i\right) \cdot \left(\log p\left(x_i\right) - \log q\left(x_i\right)\right), \tag{1.5}$$

where p and q are two distributions for which we want to calculate relative entropy. Combining this formula with exponent (for easier comparison between different results) we obtain final Inception Score definition:

$$\mathrm{IS}(G) = \exp\left(\mathbb{E}_{\mathbf{x}} D_{KL}(p(y|x)\|p(y))\right) \tag{1.6}$$

Fréchet Inception Distance is another metric based in Inception model proposed in [4] as an alternative for Inception Score. One of the drawbacks of Inception Score, as pointed out by authors, is the fact that it does not capture the comparison of generated

images to the real images. It does not refer to real data statistics when calculating final value.

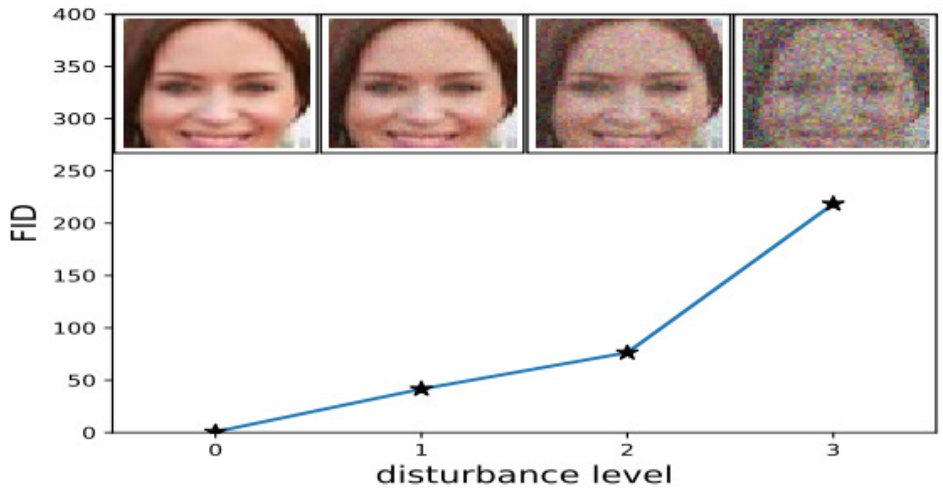

Figure 1.5: Plot of how FID scoring changes when Gaussian noise is added to the image [4].

Idea for the new metric is to use one of the last layers in the Inception model (pooling layer before classification output) to capture and encode specifics of an image. The output vector of this layer is of shape $(2048,)$ and is approximated by multivariate normal distribution. Set of these features is calculated for both real images and images generated by the model. We can denote the mean and covariance of embedded layer for generated images as, respectively, μ_r and Σ_r. Same properties for real images are denoted as μ_g and Σ_g. Final score is calculated as a distance between the two data distributions, formally defined as

$$\mathrm{FID}(r, g) = \|\mu_r - \mu_g\|_2^2 + \mathrm{tr}\left(\Sigma_r + \Sigma_g - 2\left(\Sigma_r \Sigma_g\right)^{\frac{1}{2}}\right), \tag{1.7}$$

Lower FID values indicate better generator performance, as the two distributions are *closer* to each other. This score is more robust to noise than Inception Score - if generator only outputs small number of images per class (generated images are similar), the distance value between distributions will be high.

1.2 CLIP model

1.2.1 Overview

In January 2021 OpenAI released new multi-modal model called **CLIP - Contrastive Language-Image Pre-Training**. It is a neural network trained on 400 000 000 image-text pairs - each pair is an image and its caption scrapped by OpenAI from the Internet. Main usage of the model is obtaining the most relevant text snippet for given image by using natural language embeddings and without directly optimizing for the task. CLIP

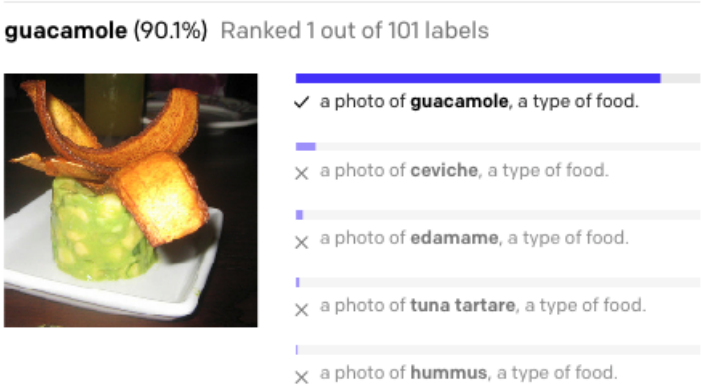

Figure 1.6: Example of CLIP prediction [13].

is an example of **zero-shot** model. That is, compared to commonly used classifiers that require custom datasets that represent target classes and don't generalize very well, CLIP can identify an enormous range of objects it has never seen before. OpenAI proves such functionality in the following table

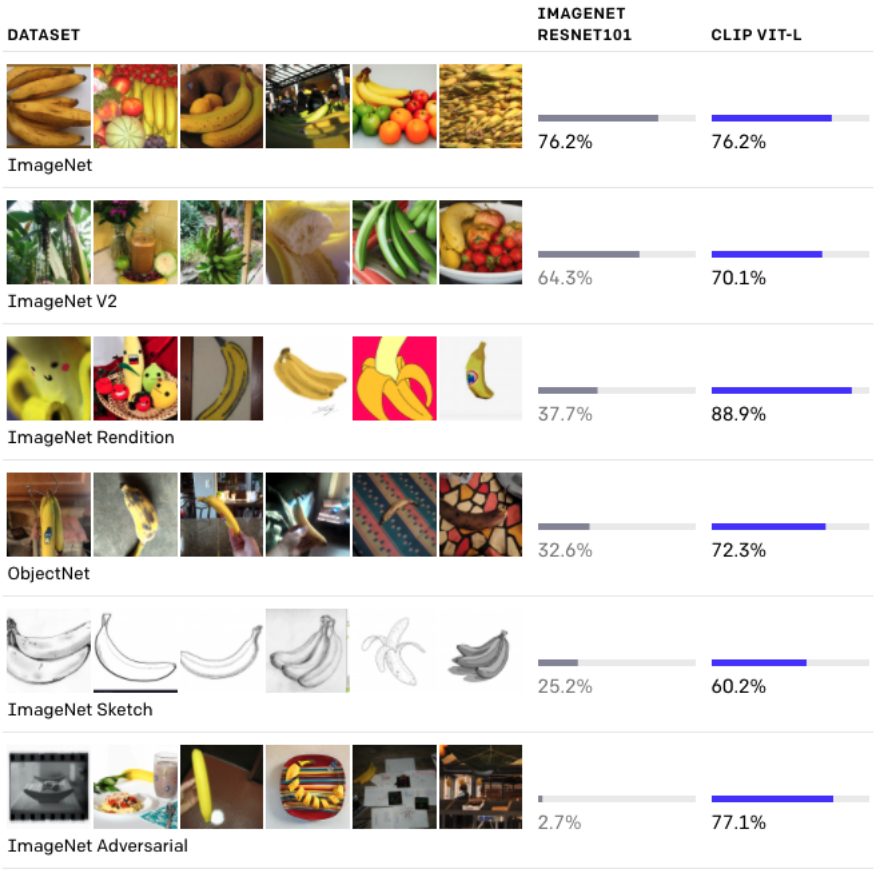

Figure 1.7: Comparison of classification accuracy for CLIP and Resnet101 models for selected datasets [13].

It compares ResNet101 model - trained on the ImageNet dataset with CLIP accuracy on different datasets. It can be seen that for the ImageNet dataset, the accuracy is identical, but for the other models CLIP clearly provides better results and hence can be viewed as better generalizing model.

1.2.2 Methodology

In order for images and text to be compared to one another, they must both be embedded. Part of the CLIP model is responsible for embeddings - it contains two encoders - ImageEncoder and TextEncoder.

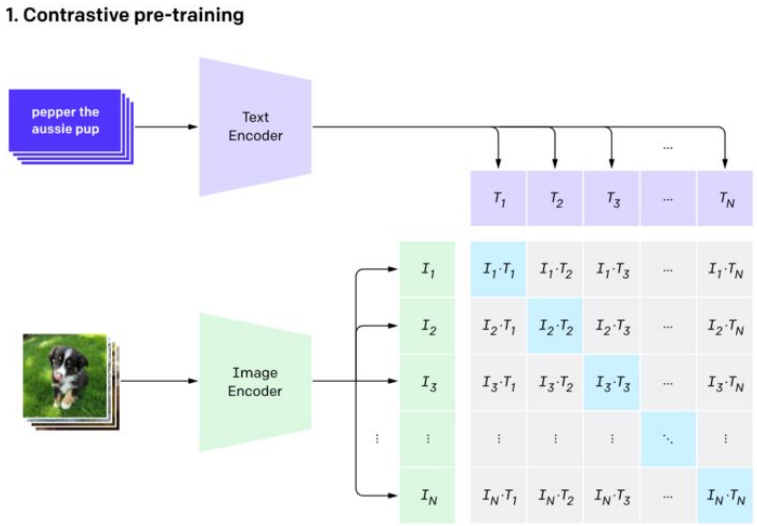

Figure 1.8: CLIP pre-trains an image encoder and a text encoder to predict which images were paired with which texts in the dataset [13].

Image and text embeddings are compared in the similarity matrix $I \times T$ using **cosine similarity**:

$$\text{sim}(\mathbf{A}, \mathbf{B}) = \frac{\sum_{i=1}^{n} A_i B_i}{\sqrt{\sum_{i=1}^{n} A_i^2} \sqrt{\sum_{i=1}^{n} B_i^2}}, \tag{1.8}$$

where $\mathbf{A}$ and $\mathbf{B}$ are two vectors representing image and text embeddings respectively. Model objective is to maximize cosine similarities for successive training (image, text) pairs and minimizing it for "negative" pairs - which means not training pairs.
One detail that is worth mentioning is that CLIP is sensitive to words used for image descriptions. Texts “a photo of a bird”, “a photo of a bird siting near bird feeder”, or “an image of a bird” all produce different probability paired with the same image:

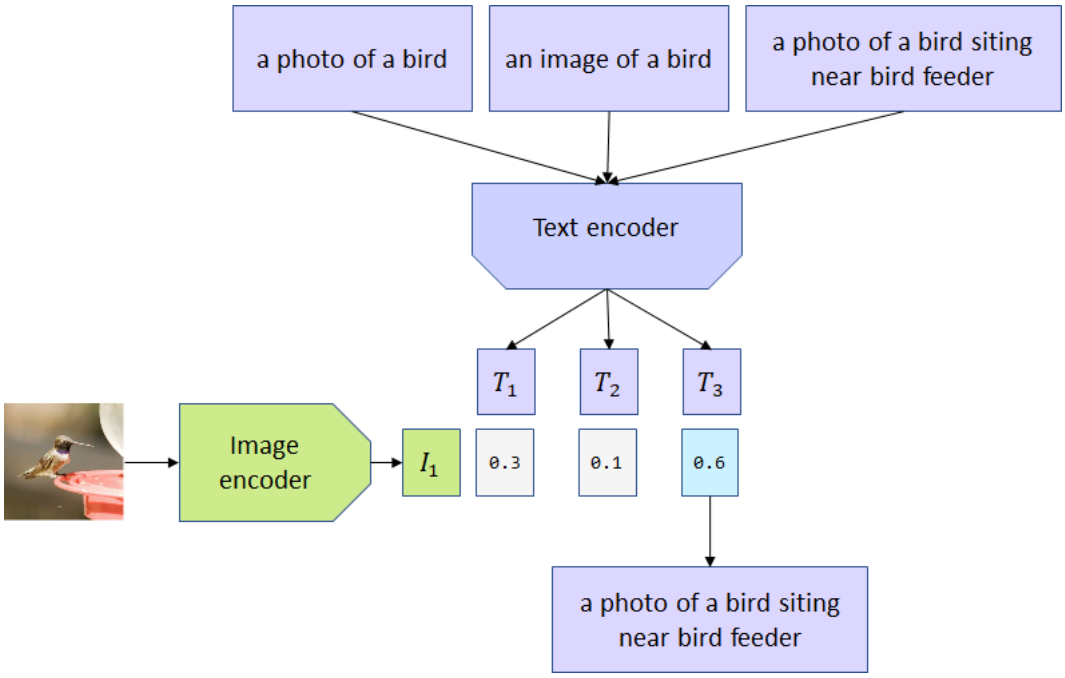

Figure 1.9: CLIP is producing different probabilities for different bird image descriptions [14].

Current results and limitations

CLIP authors are open about its limitations. CLIP struggles on more abstract or systematic tasks such as counting the number of objects and on a more complex tasks such as estimating relative distances between objects. On such datasets, CLIP is only slightly better than random guessing. CLIP also struggles with very fine-grained classification, such as telling the difference between car models, variants of aircraft, or flower species.

What's more, CLIP model itself is data hungry and expensive to train. If pre-trained model doesn't work well for you, it may be not feasible to train your own version.

While zero-shot CLIP tries to reformulate classification task, the principles are still the same. And although CLIP generalizes well to many image distributions, it still generalizes poorly to data that is truly out-of-distribution. One example of this was CLIP's performance on MNIST dataset where CLIP zero-shot accuracy was 88%. Logistic regression on raw pixels outperforms CLIP.

Ability to adapt to new datasets and classes is related to text encoder. It is thus limited to choosing from only those concepts known to the encoder. CLIP model trained with English texts will be of little help if used with texts in other languages.

Finally, CLIP's classifiers can be sensitive to wording in label descriptions and may require trial and error to perform well.

1.3 Evolutionary Algorithms

Evolutionary algorithms are a population-based heuristic methods of optimization. Algorithms from this family use computational implementations of processes related to natural selection, such as crossover, mutation and reproduction. Main idea of the algorithm is the *survival of the fittest* principle inspired by Darwinian evolution theory, where main objective is to generate more and more *fit* members of the population, while reducing the number of *weak* units. That *fitness* level is measured and described by *fitness function*, which determines the quality of each population sample.

In the following sections we will describe main algorithms of our interest that we will apply for latent search problem.

1.3.1 Genetic Algorithm

The Genetic Algorithm is one of the first methods used and defined as evolutionary algorithm. It is still used with success until today and the number of variations and different applications of the method still grows.

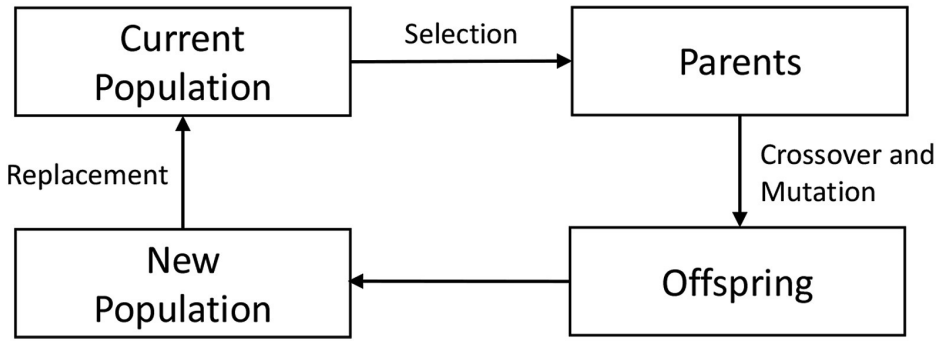

Figure 1.10: Genetic algorithm optimization loop.

Standard genetic algorithm uses several operators for optimization purposes:

1. **Crossover** - process in which units from latest population are *mixed* together at random. In this way, offsprings that come from the parents have combined features from both parents. It works for intensification and diversification of search, although it depends on the type of crossover operator and the location of the parents in the search space.

2. **Mutation** - these operators are widely regarded as introducing some random disturbance for individual units in the population. Uniform mutation replaces the value of a single decision variable by a value that is randomly selected from a space within lower and upper bound for given variable. This mainly introduces diversification and also helps to escape local optima.
3. **Replacement** - after performing crossover and mutation for given population, newly generated offspring are evaluated by the fitness function. Several (this number is usually dependent on the algorithm hyperparameters) newly created members with best score are placed in the population, the same number of worst units is removed.
4. **Selection** - the most promising units from population (members with best results regarding the fitness function) are chosen for mating. This generally promises the best chance to generate better units in the next population.

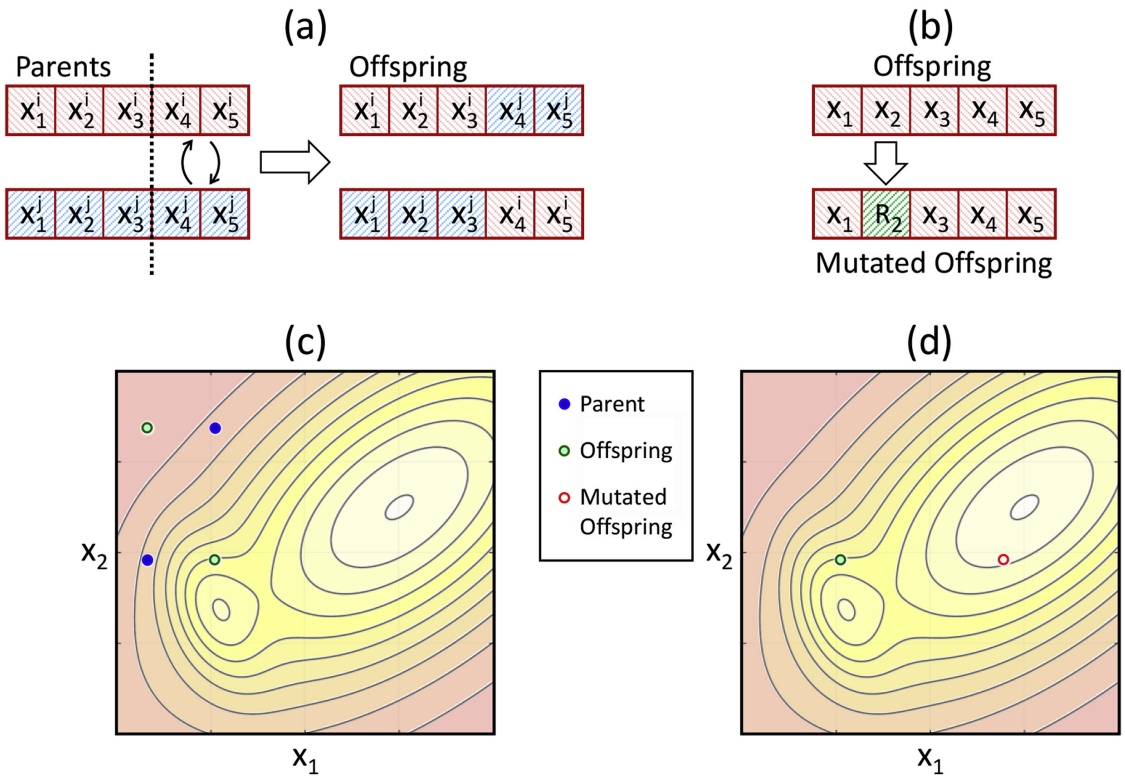

Figure 1.11: Example of crossover and mutation operations.

The algorithm terminates based on several common criteria, most often when a solution is found that satisfies minimum criteria or when fixed number of generations is reached. Below is the pseudocode for the base genetic algorithm.

Algorithm 1 Genetic Algorithm

```
1: determine objective function (OF)
2: assign number of generation to 0 (t=0)
3: randomly create individuals in initial population P(t)
4: evaluate individuals in population P(t) using OF
5: while termination criterion is not satisfied do
6:     t=t+1
7:     select the individuals to population P(t) from P(t-1)
8:     change individuals of P(t) using crossover and mutation
9:     evaluate individuals in population P(t) using OF
10: end while
11: return the best individual found during the evolution
```

Figure 1.12: Genetic algorithm pseudocode.

1.3.2 Differential Evolution

Differential evolution algorithm is a very efficient method most commonly used for optimization of function in continuous search space. It was proposed by Storn and Price in [5].

The main advantages over general genetic algorithm is more efficient memory usage, lower complexity and faster convergence.

Below we will present the mathematical formulation of the algorithm and discuss most popular versions.

Differential evolution is primarily described by three parameters: N_p - population size, C_r - crossover control parameter and F - scaling factor, also known as amplification parameter. Each member of every population is described as D-dimensional parameter vector. Each population in the algorithm can be understood as vector $\mathbf{x}_{i,g}$, where $i \in \{1, 2, ..., N_p\}$ and g stands for generation number.

Method incorporates usage of three vectors, which we will name for simplicity:

- Donor vector, which is created in the mutation step,
- Trial vector, which is created in the crossover step,
- Target vector, which is the vector of current population.

In the **mutation** step donor vector $v_{i,g}$ is produced. It is calculated by adding the scaled difference of two vectors to the third vector from the population. There are two most

Algorithm 2 Differential Evolution

```
1: determine objective function (OF)
2: assign number of generation to 0 (t=0)
3: randomly create individuals in initial population P(t)
4: while termination criterion is not satisfied do
5:     t=t+1
6:     for each i-th individual in the population P(t) do
7:         randomly generate three integer numbers:
8:         r1, r2, r3∈[1; population size], where r1≠r2≠r3≠i
9:         for each j-th gene in i-th individual (j∈[1; n]) do
10:            v_{i,j} = x_{r1,j} + F · (x_{r2,j} − x_{r3,j})
11:            randomly generate one real number rand_j ∈
    [0; 1)
12:            if rand_j < CR then u_{i,j} := v_{i,j}
13:            else
14:                u_{i,j} := x_{i,j}
15:            end if
16:        end for
17:        if individual u_i is better than individual x_i then
18:            replace individual x_i by child u_i individual
19:        end if
20:    end for
21: end while
22: return the best individual in population P(t)
```

Figure 1.13: Differential evolution DE/rand/1 pseudocode.

popular variations of mutation used in differential algorithm, one is the *DE/rand/1* version, where all three vectors used in mutation are taken at random, which allows us to write a formula for donor vector $v_{i,g}$ as

$$\mathbf{v}_{i,g} = \mathbf{x}_{r_1,g} + F\left(\mathbf{x}_{r_2,g} - x_{\mathbf{r}_3,g}\right), \tag{1.9}$$

where $r_1, r_2, r_3 \in \{1, 2, ..., N_p\}$ are randomly selected indices and F is the aforementioned scaling factor.

The other choice is the *DE/best/1* version, which chooses two random vectors to calculate the scaled value which is used to change the **best** vector $\mathbf{x}_{best,g}$ in current population, which results in more greedy version of the method

$$\mathbf{v}_{i,g} = \mathbf{x}_{best,g} + F\left(\mathbf{x}_{r_2,g} - x_{\mathbf{r}_3,g}\right). \tag{1.10}$$

After the mutation algorithm performs **crossover** step. There are two most popular crossover schemes: binomial and exponential. Crossover step is performed using rate parameter $C_r \in (0, 1)$, which determines size of perturbation of the target vector. This influences the population diversity.
In binomial crossover, the trial vector $\mathbf{u}_{i,g} = (u_{i,1,g}, u_{i,2,g}, \ldots, u_{i,D,g})$ for $i \in \{1, 2, ..., N_p\}$ and $j \in \{1, 2, ..., D\}$ is created using formula

$$u_{i,j,g} = \begin{cases} v_{i,j,g} & \text{if } rand_j \leqslant C_r \text{ or } j = j_{\text{rd}}, \\ x_{i,j,g} & \text{otherwise,} \end{cases} \tag{1.11}$$

where $rand_j$ is a random number from $(0, 1)$ which determines the probability that the j-th parameter will crossover and $\mathbf{v}_{i,g}$ is the donor vector calculated in the mutation step. Also, j_{rd} is a randomly chosen integer in the range $[1, D]$, which ensures that at least one parameter will be chosen for crossover. That ensures that the new population will be always different from previous one.

For exponential crossover scheme, let us define the indices a and b to be chosen independently and at random from $[1, D]$. These parameters are chosen for each trial vector separately. Let's denote $()_{MOD_D}$ as modulo function with modulus D. Using these we can define a set of indices

$$I = \left\{a, (a+1)_{MOD_D}, \ldots, (a+b-1)_{MOD_D}\right\}. \tag{1.12}$$

The trial vector $\mathbf{u}_{i,g} = (u_{i,1,g}, u_{i,2,g}, \ldots, u_{i,D,g})$ for $i \in \{1, 2, ..., N_p\}$ and $j \in \{1, 2, ..., D\}$ is created as

$$u_{i,j,g} = \begin{cases} v_{i,j,g} & \text{if } j \in I \text{ and } rand_j \leqslant C_r, \\ x_{i,j,g} & \text{otherwise.} \end{cases} \tag{1.13}$$

Essentially, above formula is focusing on the crossover between neighbouring vector features instead of fully randomizing the choice.
Having produced a trial vector we can proceed to the selection step. In this phase, algorithm is greedily choosing new members of the population using the *fitness function* f.

$$\mathbf{x}_{i+1,g} = \begin{cases} \mathbf{u}_{i,g} & \text{if } f\left(\mathbf{u}_{i,g}\right) < f\left(\mathbf{x}_{i,g}\right), \\ \mathbf{x}_{i,g} & \text{otherwise} \end{cases} \tag{1.14}$$

The algorithm terminates on similar basis as genetic algorithm discussed previously, when a optimal solution below certain treshold is found or when algorithm reaches some defined number of generations.

Chapter 2

Notable architectures

2.1 StyleGAN

StyleGAN is an architecture proposed by NVIDIA team in [6]. It is considered to be one of the most important publications regarding image generation and it introduces several novelties comparing to models used so far. It used several mechanisms (such as adaptive instance normalization and merging regularization) to generate highly realistic images with great resolution. It is greatly inspired by direct predecessor - Progressive Growing GAN architecture (called ProGAN), also published by NVIDIA.

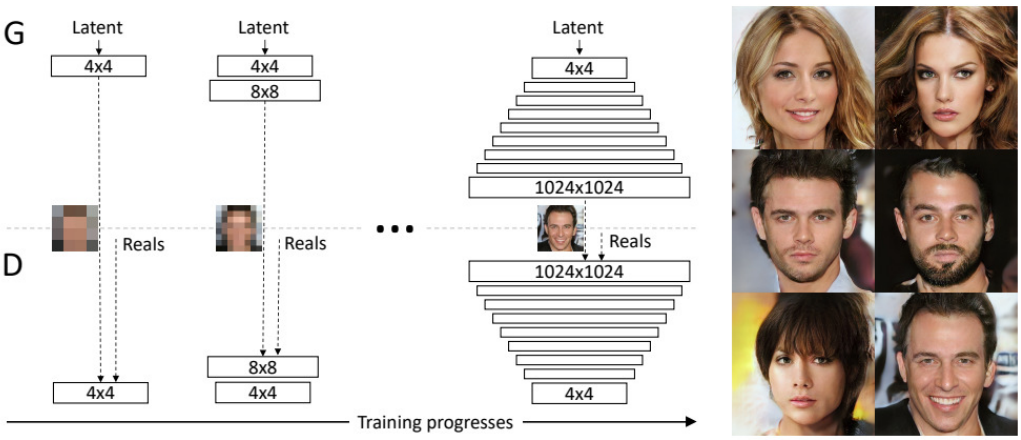

Figure 2.1: Progressive growing technique used in ProGAN.

Most important idea presented in the ProGAN architecture, utilized also in StyleGAN, is the progressive structure of learning. Volume of generated by network images is growing from small resolution (starting at 4x4 pixels) to high resolution (up to 1024x1024 pixels) by upsampling. This training principle helps the network to solve simpler task before attending to generate a full-resolution image. It has been proven

to help with stability of the training and reduce drastic abnormalities in final image.

2.1.1 Architecture overview

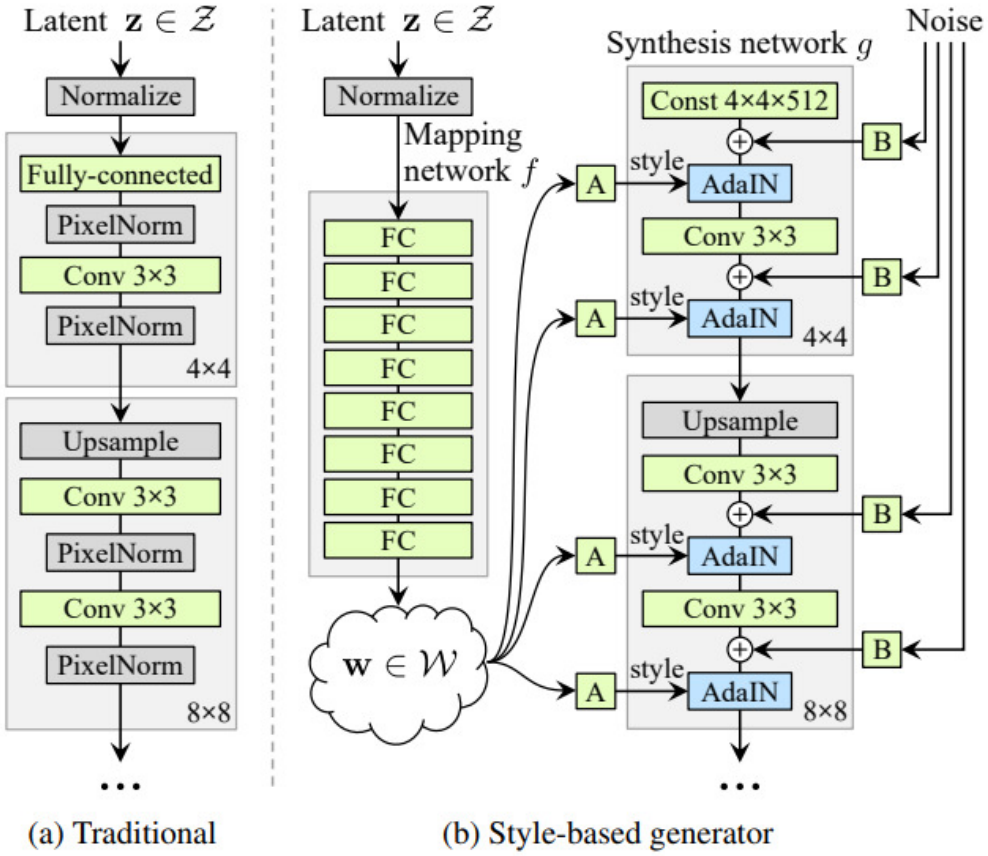

Figure 2.2: ProGAN and StyleGAN networks comparison.

2.1.2 Mapping network

In the StyleGAN architecture authors introduced a intermediate layer between an input (latent vector $z \in \mathbb{Z}$) and the network called mapping layer (fig...). It works by applying 8 fully connected layers to the input and therefore encoding it as a new vector $w \in \mathbb{W}$. Main purpose of this procedure is to have better control over generative power of the model by separating elements of the vector that will be responsible for different image features.

A common problem for generative models is a phenomenon called **feature entanglement**. We can consider a scenario where training is done on a dataset of human

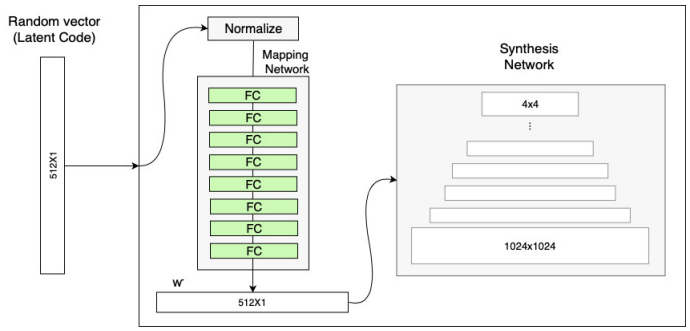

Figure 2.3: Mapping network of StyleGAN.

faces. It is very likely that most of the women in the dataset will have long hair and most men - short hair. This would result in the entanglement of *hair length* and *gender* features. Therefore, when latent vector is manipulated in order to change the hair length - the model will also change the gender of a person on the image, as it is associating these two occurencies as bounded together. The mapping layer is separating these features, allowing to change different elements of new vector w without losing the integrity of an image.

2.1.3 Adaptive Instance Normalization

In the traditional generator, latent code is introduced to the network only in the first layer. The authors of StyleGAN are using the vector w produced via mapping network to steer the style of an image at each convolutional layer by using **Adaptive Instance Normalization (AdaIN)** technique.

$$\mathrm{AdaIN}\left(\mathbf{x}_i, \mathbf{y}\right) = \mathbf{y}_{s,i} \frac{\mathbf{x}_i - \mu\left(\mathbf{x}_i\right)}{\sigma\left(\mathbf{x}_i\right)} + \mathbf{y}_{b,i}, \tag{2.1}$$

The middle part of the equation is the **Instance Normalization (IN)**. Each channel of the convolution layer is normalized. Values $\mathbf{y}_{s,i}$ and $\mathbf{y}_{b,i}$ are calculated from the vector v using fully-connected layer and correspond to A on the figure-main one. These can be understood as scale and bias; these values are used to translate the information from vector w to a feature map generated by convolution.

Adding this method of including latent vector at every step of network computation resulted in drastic improvement of network's performance which can be see in the table below.

Figure 2.4: Example of AdaIN application for style transfer.

	Method	CelebA-HQ	FFHQ
A	Baseline Progressive GAN [30]	7.79	8.04
B	+ Tuning (incl. bilinear up/down)	6.11	5.25
C	+ Add mapping and styles	5.34	4.85
D	+ Remove traditional input	5.07	4.88
E	+ Add noise inputs	**5.06**	4.42
F	+ Mixing regularization	5.17	**4.40**

Figure 2.5: Mapping network of StyleGAN.

2.1.4 Style mixing regularization

As additional technique of regularization and method to differentiate the generated images further, a **style mixing** approach was introduced by the authors. The main idea is to use not one but two (or more) latent vectors w_1, w_2 (obtained from mapping of z_1, z_2) to generate the final image. The way in which mixing is introduced is fairly simple; up to certain point in the architecture vector w_1 is used for style control and from crossover point vector w_2 is used. Depending on the place of crossover, final image obtains different characteristics from each image.

2.2 StyleGAN2

Significant improvements of the StyleGAN architecture were proposed in late 2019. Publication revolved mainly around the problems which emerged during StyleGAN generator. It has been noticed that several parts of the network cause imperfections in the final images, which are called *artifacts*. Two main types of artifacts were formulated in the paper:

- **Water-droplet artifacts** - the blob-shaped characteristics that resemble water-droplets are visible in various places in the final images. It might not be obvious while looking at the image, but it is very visible in the intermediate feature maps produced by generator. This artifacts starts to appear around 64x64 pixels resolution and gets stronger with higher resolutions.
- **Phase artifacts** - output images show strong location preference for several features e.g. facial features like teeth or eyes. This causes some of the features to remain unchanged when major components of the image such as pose or rotation are vastly different.

Figure 2.6: Water droplets artifact and its effect on feature maps.

2.2.1 Architecture overview

2.2.2 Revisiting Instance Normalization

The water-droplet effect was speculated to be a side effect of AdaIN method applied in the style blocks. Authors pointed out that this type of normalization affects each feature map separately (works independently for every channel) and potentially destroys meaningful information that is included in the differences between feature maps values.

Figure 2.7: Phase artifact. Blue line helps to visualize that teeth are staying in the same place even with changing a significant feature of image such as rotation of the face..

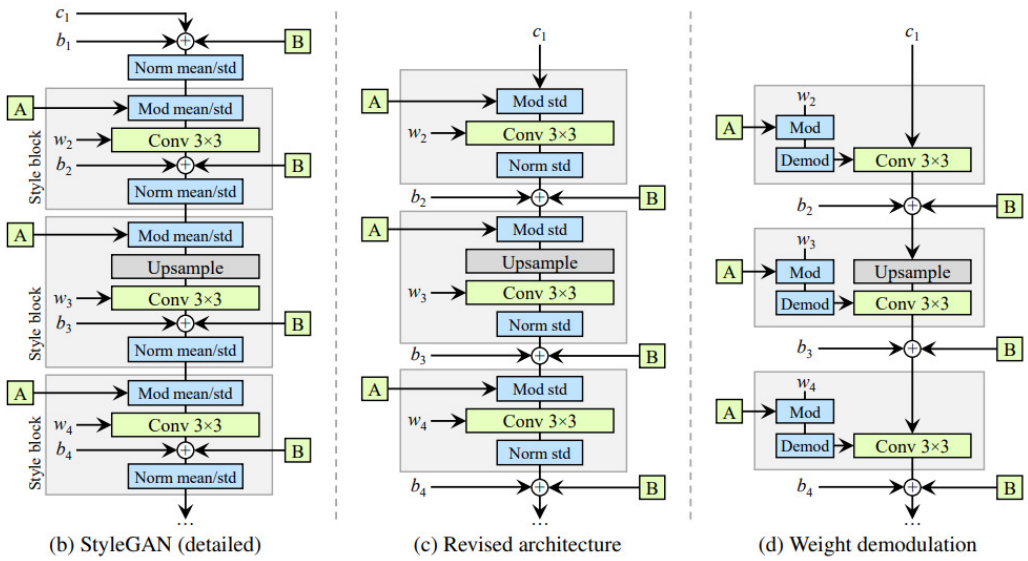

Figure 2.8: Visual inspection of where the gaussian noise tends to be the most active.

To address this problem, significant changes to the architecture were proposed.

As seen on the image above, several things changed in the network:

- Only standard deviation is modified for each feature map, modification of mean was deemed redundant as the effects of this operations were not meaningful for the network. Removing this part made the model simpler,
- Noise addition was removed from the style block and instead applied inbetween the blocks. This was mainly done to prepare the network for weight modulation,
- Input vector c is fed to the network directly, without normalization and applying

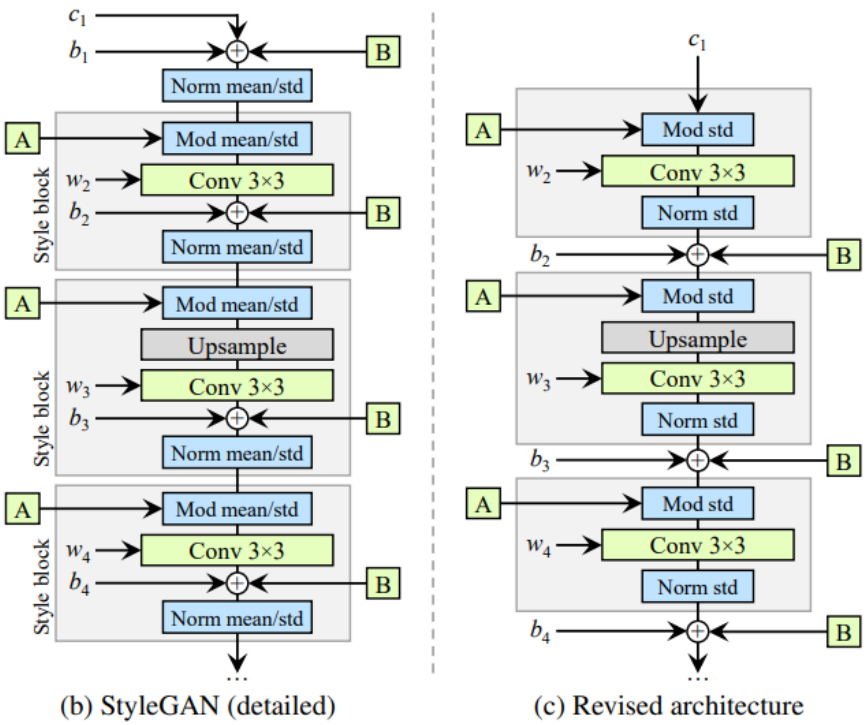

Figure 2.9: (b) shows the original StyleGAN architecture. The AdaIN fucntion is shown as combination of normalization and modulation operations. (c) shows the revised model with changes in the network.

noise.

All of these steps were also necessary to introduce the main idea for handling water-droplets artifact problem - **weight demodulation**.

2.2.3 Removing Progressive Growing

StyleGAN2 uses different resolution feature maps that are produced in the base network and uses the ResNet like skip connections to incorporate lower resolutions maps to the final output. This change can be viewed as quite drastic - the whole concept of base network was changed, but it proved to be a necessary step in order to mitigate the *phase artifact* effect.

2.3 BigGAN

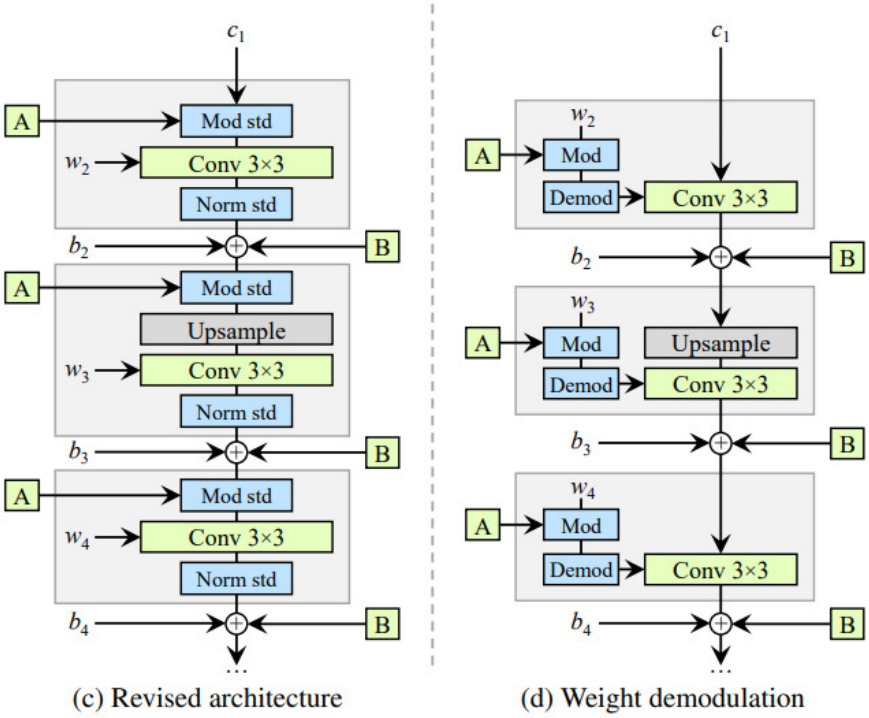

Figure 2.10: (b) shows the original StyleGAN architecture. The AdaIN fucntion is shown as combination of normalization and modulation operations. (c) shows the revised model with changes in the network.

Chapter 3

Framework description

3.1 Overview

The architecture of solution that we are exploring in this work consists of four main components:

1. Pre-trained generative model based on Generative Adversarial Network architecture,
2. CLIP model,
3. Evolutionary optimization algorithm,
4. Evaluation using classification network.

Graph below shows the flow of data and describes the overall framework architecture:

Description of the flowchart:

1. First, text is provided by the user,
2. Introduced text is encoded using pre-trained CLIP model.

Next steps can be considered as a 'optimization loop':

3a. Algorithm is performing optimization step,

3b. Optimized population of samples (vectors) is serving as an input for generator which produces images,

3c. Generated images are evaluated by fitness function (in our case, similarity function).

After completing this process, post-processing part takes place:

4. Output images are passed for an evaluation using classification network and similarity metric.

We consider StyleGAN2 architecture as the main choice for a generative model in this solution. Main advantages of that choice are:

- It is widely available as a pre-trained structure; it is public and open-sourced for both generative and discriminative parts of the architecture.
- It consists of several class-based dedicated models (such as StyleGAN2-car or StyleGAN2-horse). It allows for experimentations with different types of images.
- It is still considered a state-of-the-art model regarding the quality of produced images and was trained using huge datasets of images.

As of optimization algorithm, we used two algorithms described in previous chapters - *genetic algorithm* and *differential evolution*.

Chapter 4

Experiments

4.1 Examples and observations

4.2 Genetic Algorithm and Differential Evolution

Both of the algorithms presented in this work are population based and work applying similar techniques and concepts. Even though, by testing different scenarios we noticed that several patterns emerged for the generating process using both of these algorithms. Differential evolution algorithm starts converging slower than genetic algorithm. It is especially visible in the first generations of the algorithms e.g. 10th generation. Images produced by generator after steering with genetic algorithm tend to be visually (and according to the metric) closer to the target text. First figure below shows this occurrence.

The input phrase used to generate was '***a yellow car in the city***'. Dedicated model trained on car images was used - StyleGAN2-car. Population obtained from genetic algorithm after 10 generations already has some acceptable units based on the input phrase. Cars are yellow (some of them deformed but the color is correct) and some of them are in the urban space. That means that genetic algorithm already steered the latent vector into the embedding of information about yellow color, car and the city.

On the other hand, differential evolution did not process the information about color yet - produced cars are random in that subject.

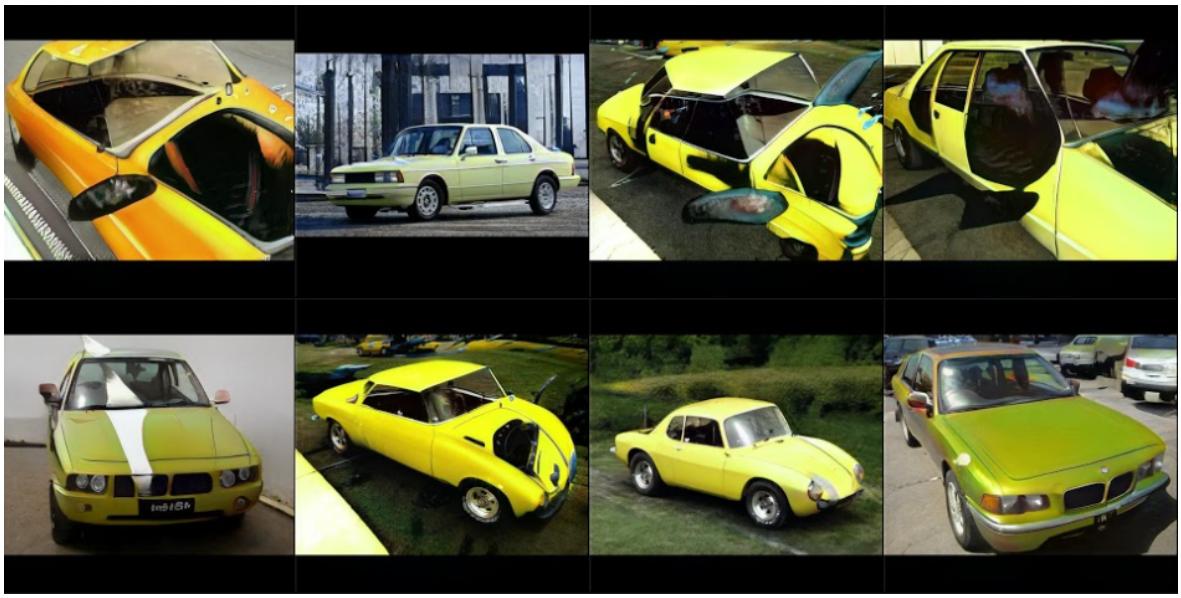

(a) genetic algorithm

(b) differential evolution

Figure 4.1: 10th generation of evolutionary algorithms traversing the latent space.

(a) genetic algorithm

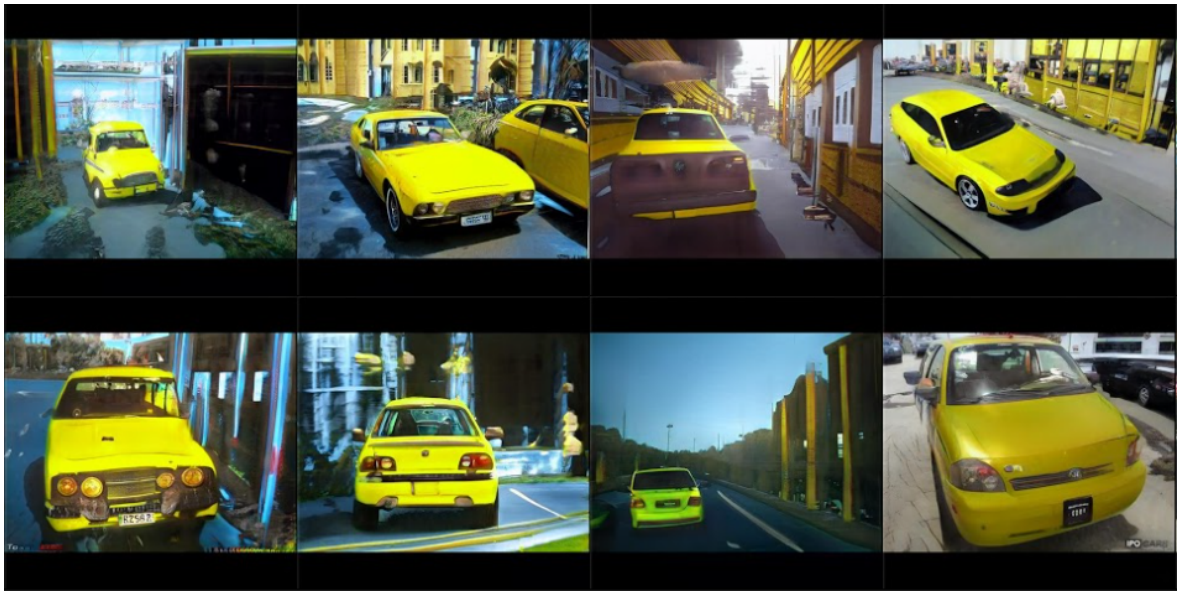

(b) differential evolution

Figure 4.2: 100th generation of evolutionary algorithms traversing the latent space.

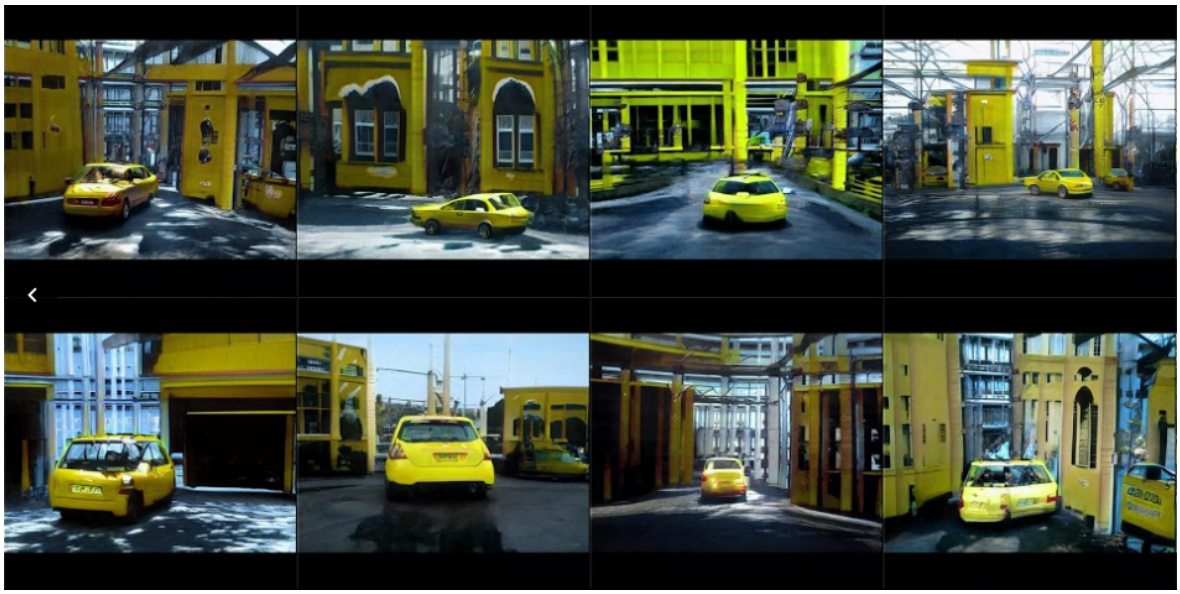

(a) genetic algorithm

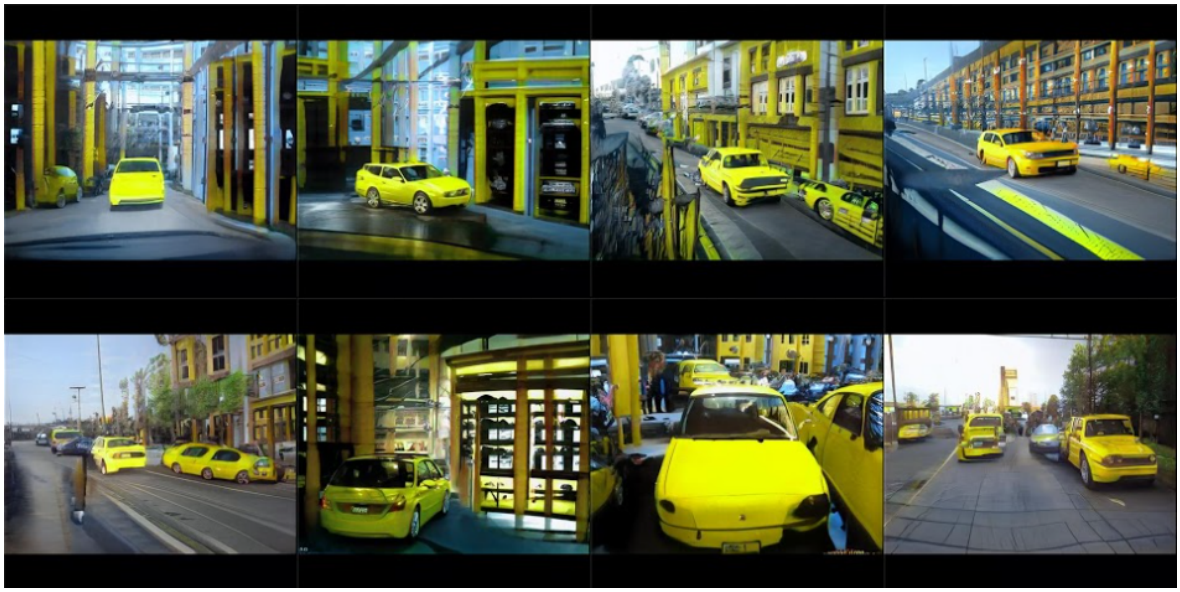

(b) differential evolution

Figure 4.3: 200th generation of evolutionary algorithms traversing the latent space.

Interestingly, we can notice that model is not comprehending the input phrase with the human-like ability - one of the examples would be 'leaking' of the context in the phrase. For instance, images from the final generation (from both algorithms) of the phrase 'a yellow car in the city' are visibly containing a lot of yellow color beside the color of the car. From human perspective, background and surroundings of the yellow car should remain arbitrary in terms of color, since only the car is supposed to be yellow according to the phrase. Generator is feeling more confident about the produced image

when yellow color is cascaded on the buildings and objects around the car. Moreover, this type of model behaviour is amplified when bright colors are used in the input phrase (such as yellow, light green).

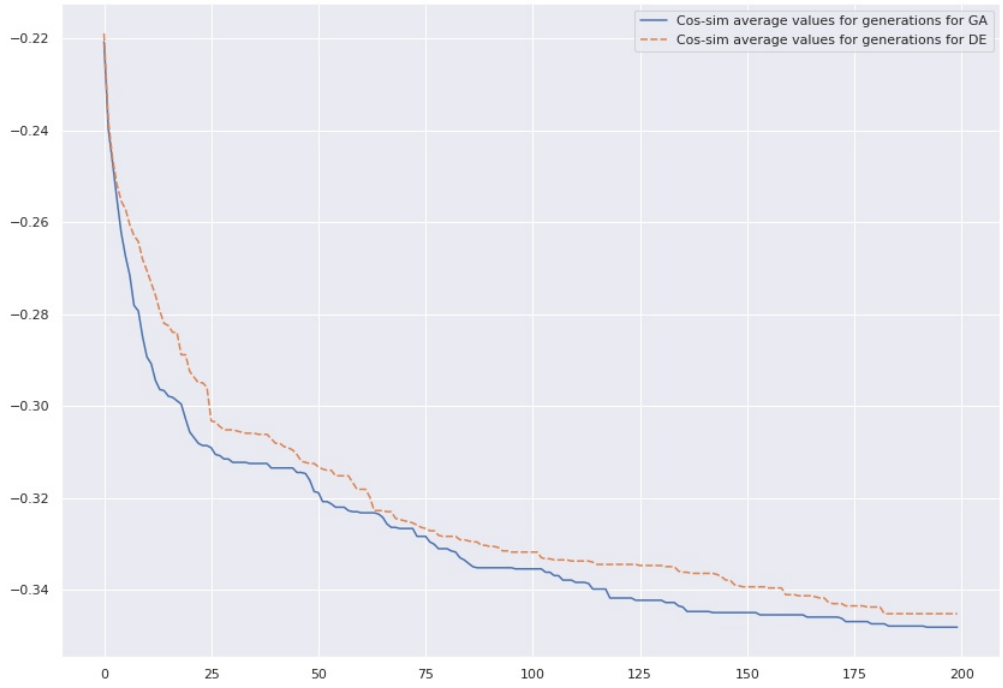

Figure 4.4: Plot of reversed cosine similarity values for generations from 0 to 200. Orange line presents differential algorithm while blue line shows genetic algorithm.

(a) genetic algorithm

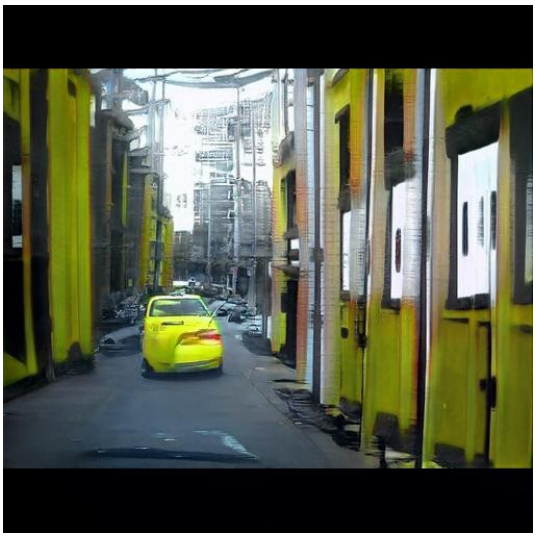

(b) differential evolution

Figure 4.5: Final images (with best score) produced by algorithms.

One of the benefits and features of using a population based algorithm for image generating is the fact that many 'similar' in terms of quality pictures are produced. The final images taken from the model have certain visible flaws - the city seems to be rendered in acceptable manner but the cars are somewhat deformed. The good part of using whole population as the output of the model is that a human can objectively choose the best image from the last produced generation. It is vital given the fact, that last images are usually close to each other in terms of scoring (which means that choosing the single final image is not based on strong decision making) but present vastly different scenarios for the input phrase.

Another example was produced by using the StyleGAN2-ffhg model. It is a model that was trained on face images and it is dedicated for that usage. The phrase used to generate below images was '***a blond girl with a smile***'.

4.3 Cosine-Similarity analysis

Another aspect that we decided to analyze is the behavior of cosine-similarity in the context of our model. This function is used in our flow in two places:

- as loss function in CLIP model,
- as loss function in evolutionary algorithms.

The most important application of *cos-sim* seems to be the ability to determine how similar according to the model the input phrase and the generated image are. Recall that *cos-sim* takes values in the range $[-1, 1]$, where 1 means that the compared vectors, image and phrase embeddings, are exactly the same. In order to check if cos-sim also reaches values close to 1 in our model, we generated a few images and checked what cos-sim was assigned to them. Let us see them:

"a car": 0.331

"a yellow forrest": 0.329

"clock": 0.313

Based on the above examples (as well as other tests performed during the research), we noticed that *cos-sim* in our solution usually oscillates in the range of 0.2 - 0.4. We see that even in obvious cases, such as the phrase "a car" - *cos-sim* is only 0.331.
We observed similar behavior during our research on CLIP model - many users noticed such regularity in their tests. Although it seems that *cos-sim*, which we determine for a pair of image-query in our solution, cannot be interpreted for a single image, we noticed from our work on evolutionary algorithms that *cos-sim* may be used as a metric comparing different images generated for the same query. Let us look at the following examples:

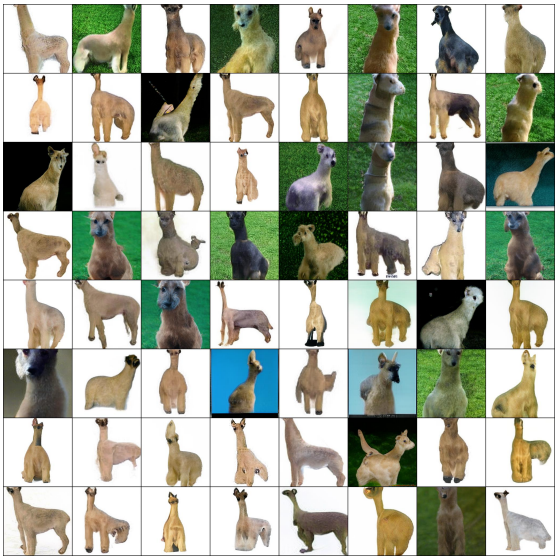

The generation from the genetic algorithm for *llama* input phrase, sorted by *cos-sim* from the top left corner - we can see that the further away the photo deviates slightly more from the given phrase.

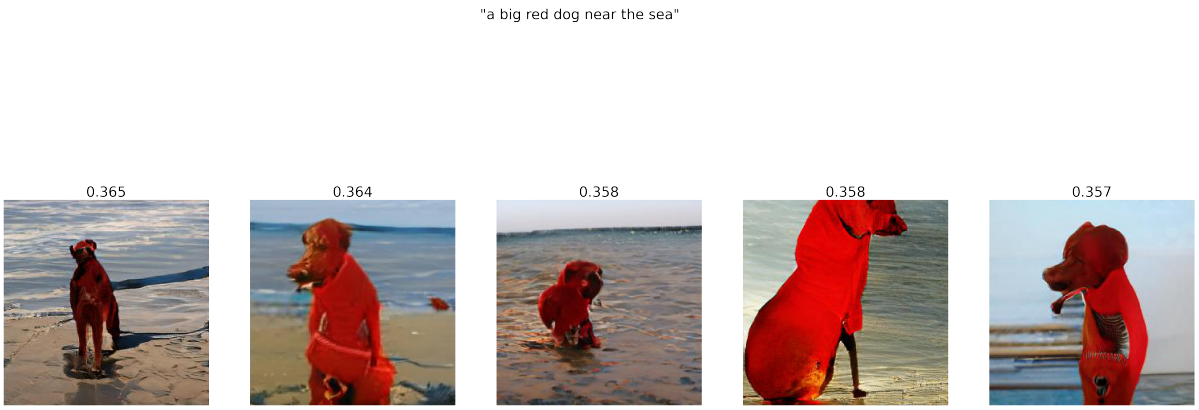

Five images generated as results of the genetic algorithm we have implemented. We

can see that *cos-sim* values differ only on decimal parts, but we can see that images with higher *cos-sim* better reflect slightly better the given phrase.

In summary, we believe that although the *cos-sim* we obtain from the CLIP model learned by OpenAI is spanned by $[0.2, 0.4]$ and not $[-1, 1]$ as in the definition, we can use this function as f. loss in our solution, or a metric to compare images for the same query.

Chapter 5

Evaluation

In order to evaluate the model we described, we decided to see if the images we generated would be able to *fool* the classifiers learned on popular datasets. We took two famous and widely used datasets as our benchmarks.

CIFAR10

CIFAR-10 dataset consists of 60000 32x32 color images in 10 classes, with 6000 images per class. There are 50000 training images and 10000 test images. The classes are mutually exclusive. Below are the classes in the dataset, as well as 10 random images from each:

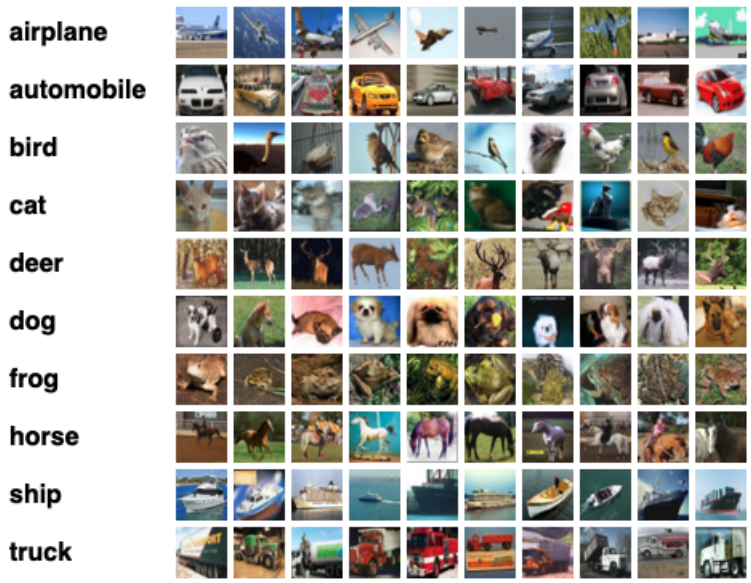

Figure 5.1: Examples from CIFAR10 dataset. [10].

CIFAR10 dataset can be downloaded from [10].

ImageNet

ImageNet dataset contains 14 197 122 hand-annotated images. Since 2010 the dataset is used in the ImageNet Large Scale Visual Recognition Challenge (ILSVRC), a benchmark in image classification and object detection. ImageNet contains more than 20000 categories. This dataset is especially useful in many evaluation cases because it contains general groups of objects (such as *balloon* or *strawberry*) as well as detailed categories e.g. dogs' breeds names like *rottweiler* or *Old English sheepdog*.

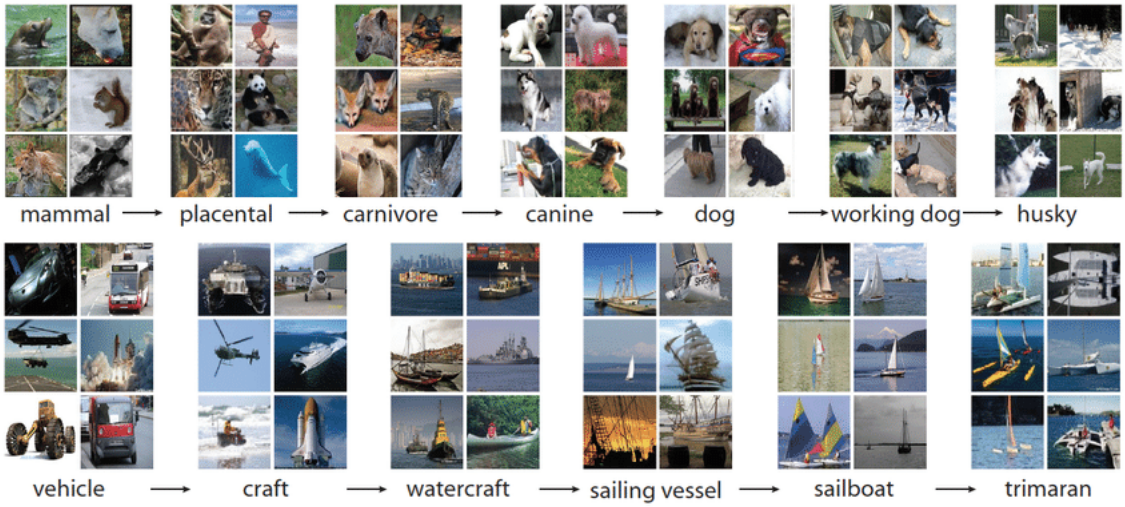

Figure 5.2: Examples from ImageNet dataset [17].

Dataset can be downloaded from [11].
Having selected datasets, we chose classifiers trained on them with high accuracy scores:

- CIFAR-10 CNN Classifier [15] - with $\sim 85\%$ accuracy.
- ImageNet - ResNet-50 Classifier [16] - with $\sim 76\%$ accuracy.

For evaluation purposes, we generated fixed number of images for selected classes from both datasets (based on the class names), and then reported what accuracy they achieved when passed through the corresponding classifiers.
For the CIFAR10 dataset we will generate images for each of the 10 available classes: **[airplane, automobile, bird, cat, deer, dog, frog, horse, ship, truck]**.
For the ImageNet dataset, we chose 10 classes each of them coming from different domain for variety purposes:

[llama, cash machine, hammer, miniskirt, pirate, shopping cart, wall clock, ice cream, banana, Kerry blue terrier]

Both evaluations were performed using intentionally selected model, algorithm and parameters settings:

- GAN model used - **DeepMindBigGAN256**
- Evolutionary model used - **GA**
- Population size - **64**
- Number of model repetitions - **8**
- Number of images generated per class - **512** = 512 = 64

5.1 CIFAR10

We present results of our evaluation in the form of the following table.

Class	Positive	Negative	Accuracy (%)
AIRPLANE	476	36	92.97
AUTOMOBILE	88	424	17.19
BIRD	12	500	2.34
CAT	177	335	34.57
DEER	0	512	0.0
DOG	255	257	49.8
FROG	39	473	7.62
HORSE	64	448	12.5
SHIP	60	452	11.72
TRUCK	97	415	18.95
TOTAL	**1268**	**3852**	**24.77**

The *positive* column informs about the number of images generated by the model that were classified correctly, and *negative* column yields the number of incorrectly classified images. From the summary of the experiment we notice that almost 25% of images generated by the model were classified correctly across all 10 classes. For this type of dataset, it is more informative to look at the results on the class basis. For most of the

classes the accuracy is way below 50%. Model had most difficulties with classes like *deer*, *bird* and *frog*. On the other side, *airplane* class had a very large score 90%.

Airplane

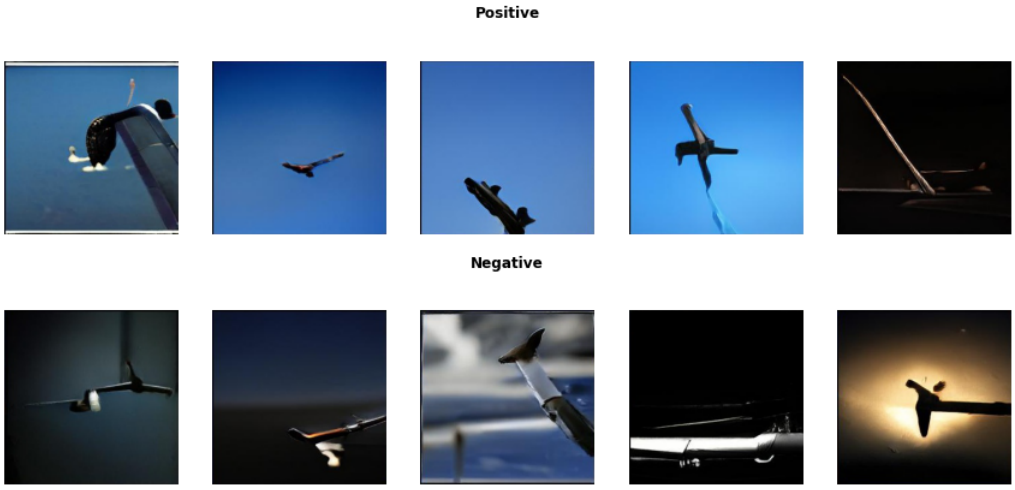

We see that the generated images of the *airplane* mostly show its wing against the sky. We can surmise that the classifier was right so often on the *airplane* images we generated, because they included the blue sky.

Dog

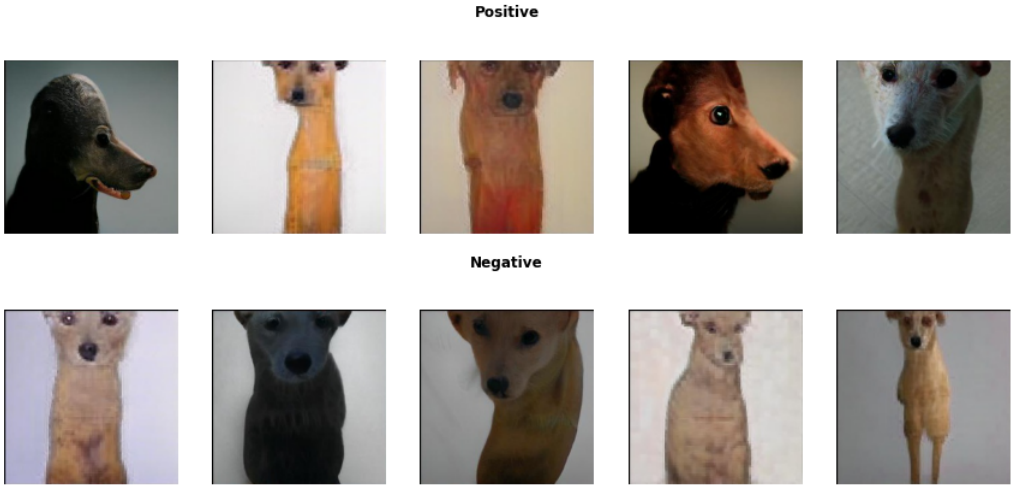

It's hard to see a feature that distinguishes correctly and incorrectly classified images in the *dog* class. Instead, it can be seen that the *dog* images generated by the model are quite readable. Later in the chapter we will look at what other classes this class was confused with.

Deer

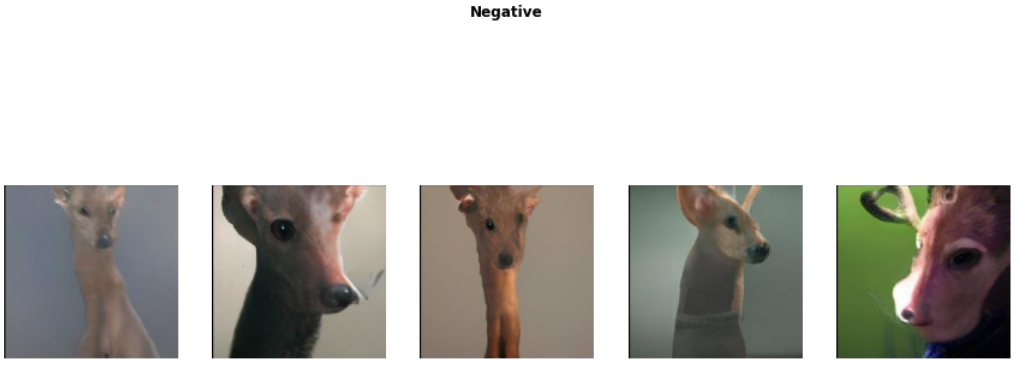

Deer class was not even once classified correctly. We can see that the generated *deers*

resemble *dogs* with some element that may represent antlers. We suspect that the model failed this task because the GAN network we used was trained on the Imagenet dataset, which does not contain images containing deers. Examples from other classes are presented in Appendix 1 of this paper.

Let us now analyze which classes the images we generated were confused with. To do this let's look at the following confusion matrix. Of course, in order to fully *fool* the

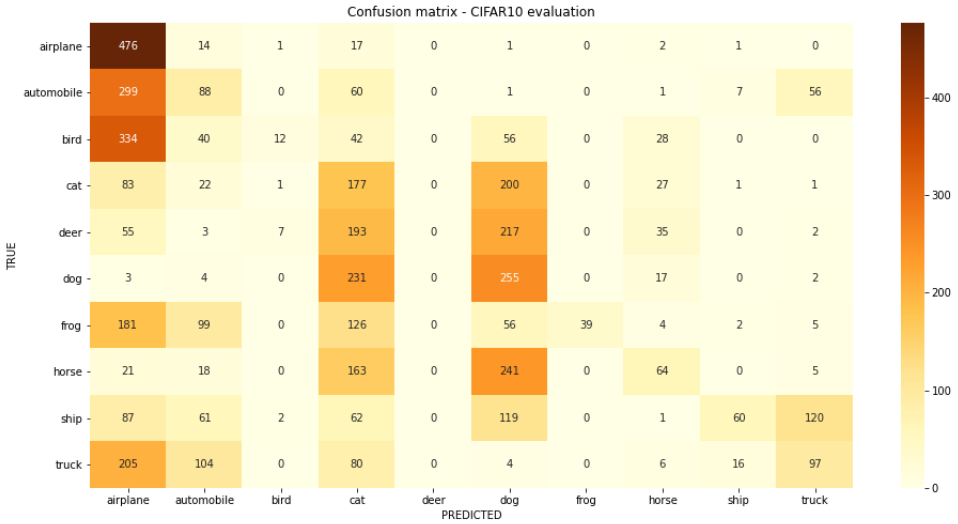

classifier with our generated images - we would expect only zero values in the above matrix except for the diagonal starting at the upper left corner. Let's present what we noticed in the matrix.

1. Many classes were mistaken for the *airplane* class - including *automobile*, *truck*, and *bird*. The mistakes in the classes *automobile* and *truck* can be explained by the fact that all 3 classes depict some kind of machine, while the problem with the class *bird* is in our opinion due to the fact that the pictures of this class also often contain a generated sky (blue background).
2. The matrix shows a clear concentration of darker color at the intersection of *cat*, *deer*, *dog* and *horse* classes. This is probably due to the fact that, as we noted earlier - the ImageNet dataset that is the "template" for the BigGAN network we are using contains many images of *dogs* and *cats*, and therefore biases the results towards them.

5.2 ImageNet

Before conducting the experiment, we intuitively predicted that the results should be at least slightly better than the results from the evaluation on the CIFAR10 dataset. This is mostly an effect of the fact that ImageNet is the basis of the BigGAN network that we use in the evaluation. The results of our evaluation are as follows. We can

Class	Positive	Negative	Accuracy (%)
BANANA	111	401	21.68
CASH MACHINE	124	388	24.22
HAMMER	141	371	27.54
ICE CREAM	3	509	0.59
LLAMA	36	476	7.03
MINISKIRT	220	292	42.97
PIRATE	5	507	0.98
SHOPPING CART	125	387	24.41
WALL CLOCK	146	366	28.52
KERRY BLUE TERRIER	253	259	49.41
TOTAL	**1164**	**3956**	**22.73**

see that we were able to fool the ResNet50 classifier nearly 23% of the time, which is lower than for the CIFAR10 dataset. However, two observations should be taken into account:

1. Imagenet dataset is significantly larger (more than 20,000 categories compared to 10 in CIFAR10)
2. ResNet50 classifier on the ImageNet dataset has an accuracy of 76%.

Let us now analyze the selected classes. For each of them we will present examples of correctly and incorrectly classified generated images, as well as a graph showing with which classes the given class was most often confused. Of course, examples of images for other classes can be found in Appendix 2.

Kerry Blue Terrier

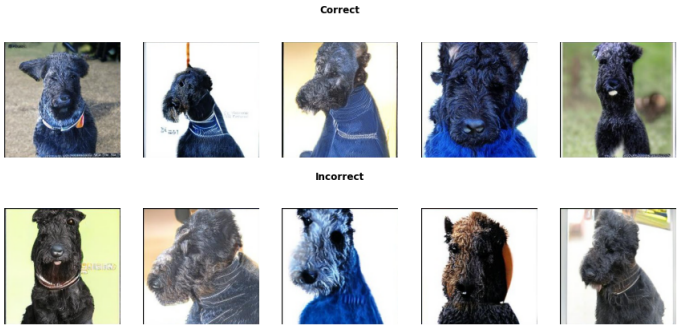

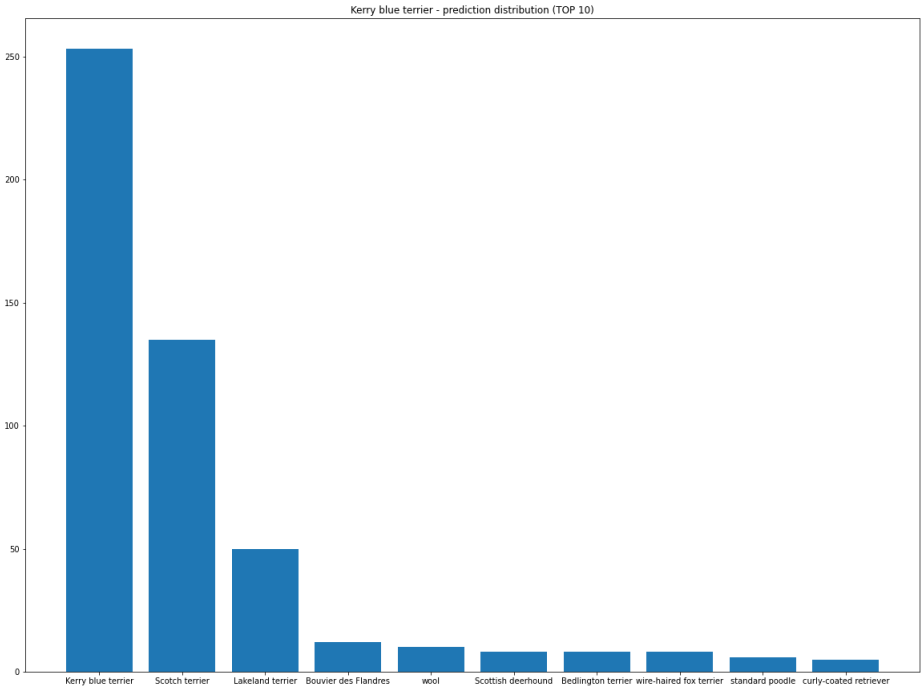

At first glance, it is clear that the images in both groups represent dogs - it is hard to judge empirically why the images in the bottom row were misclassified. However, we can make another observation - there is a noticeable problem with the context of the input query in this case - class name - *Kerry blue terrier*, which is encoded by the CLIP model. Specifically, the word *blue* is part of the dog's breed name, but when we embed the query in the model, we lose this information and experience a "leakage" of the color blue throughout the images creating, in this case, a blue dog. Analyzing the barplot

provided, we can see that in most cases our images generated for the query "Kerry Blue Terrier" were confused with other dog breeds including often other terriers. Therefore, we can conclude that if we had evaluated our model on groups of classes-for example - dogs - the accuracy of the model could have been much higher.

Llama

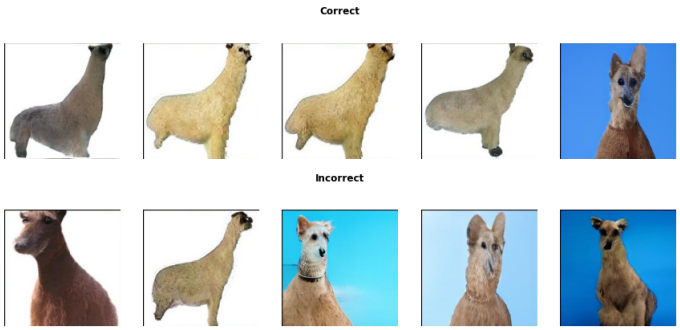

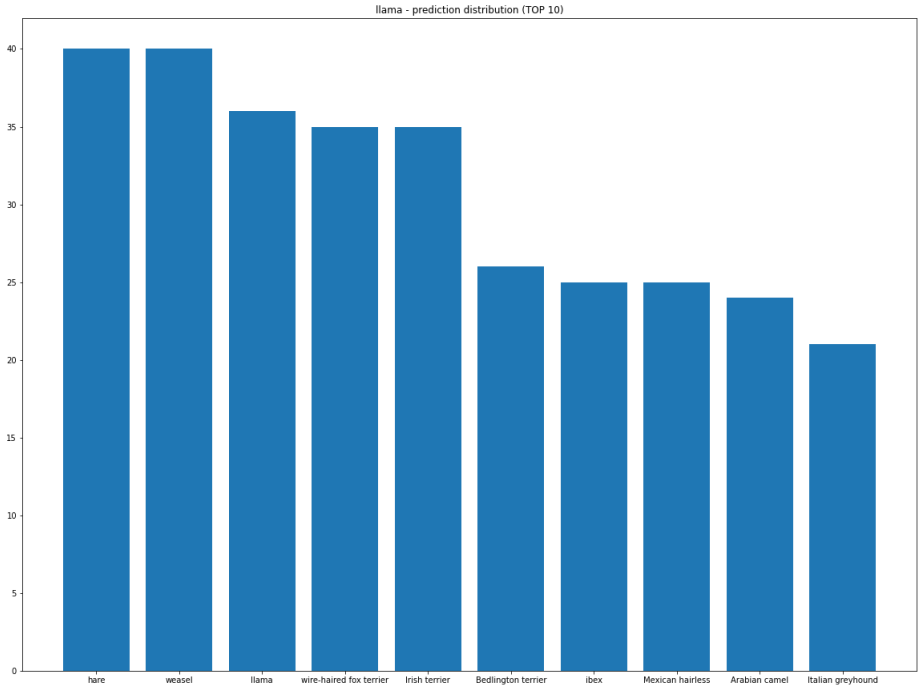

The *llama* class has a very low accuracy - 7% - in our evaluation. Here we can see a noticeable difference between correct and incorrect images - while the top row resembles the shape of a *llama*, in the bottom row we see, similarly to the section on CIFAR10

evaluations - a bias resulting probably from too many dog images in the BigGAN model training set.

Chapter 6

Summary

Chapter 7

Appendix 1

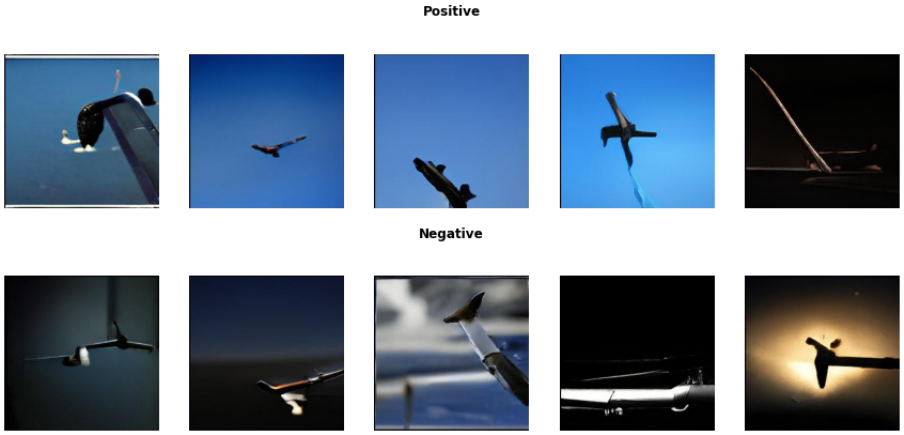

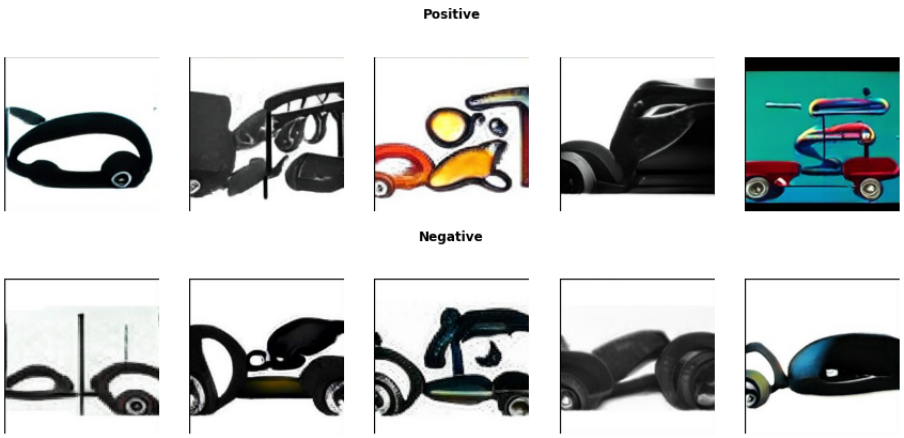

Positive

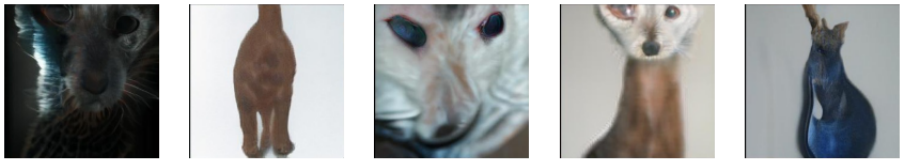

Negative

Positive

Negative

Negative

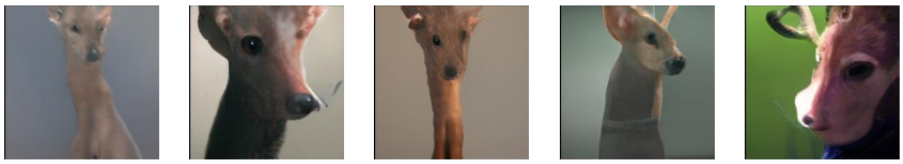

Positive

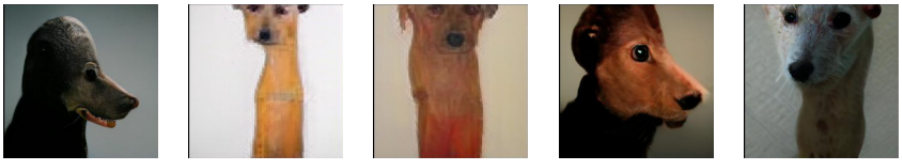

Negative

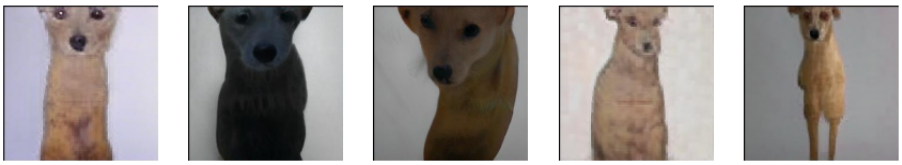

Positive

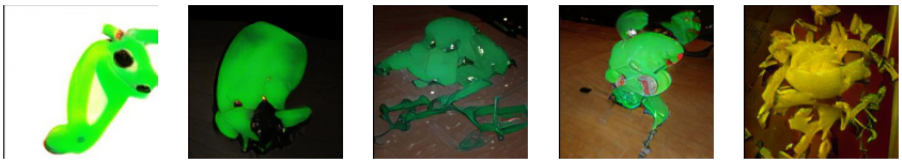

Negative

Positive

Negative

Positive

Negative

Positive

Negative

Chapter 8

Appendix 2

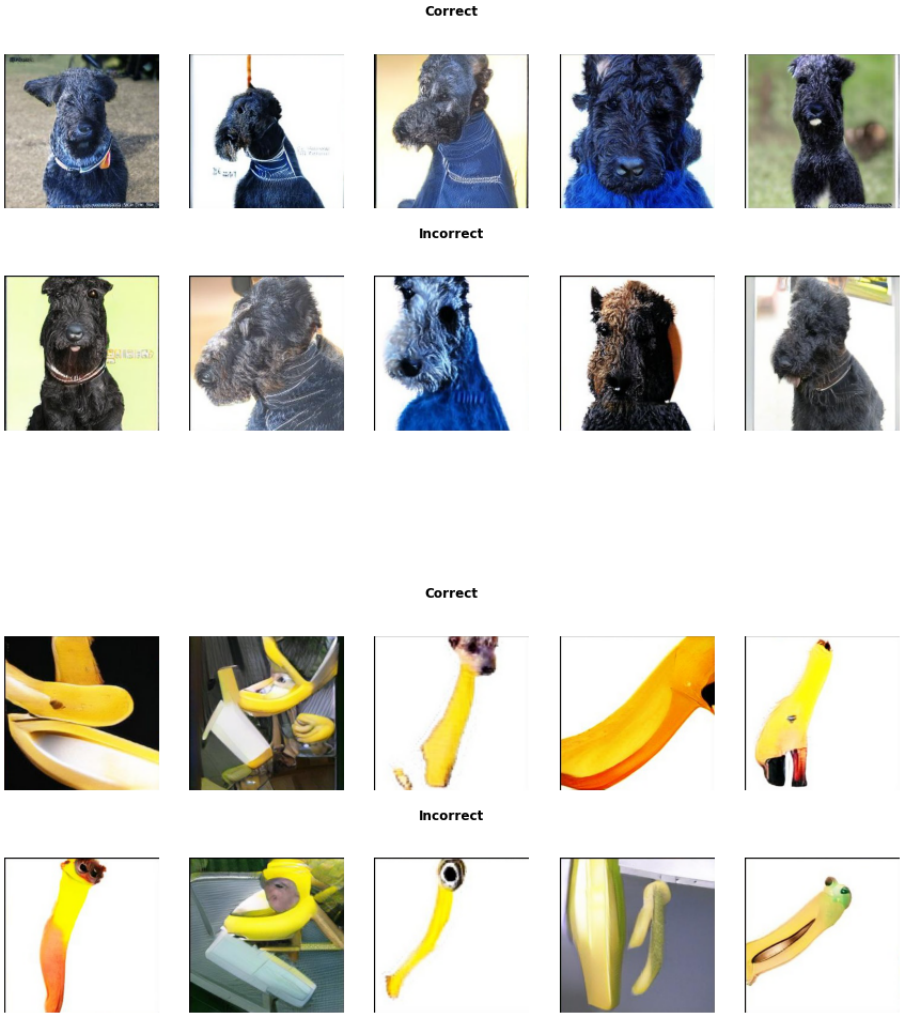

Correct

Incorrect

Correct

Incorrect

Correct

Incorrect

Correct

Incorrect

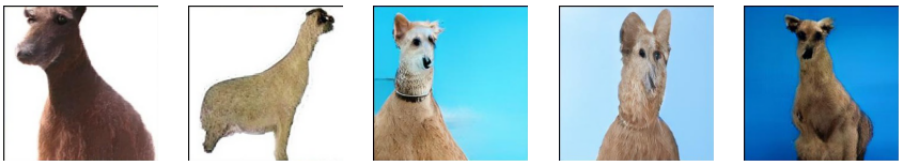

Correct

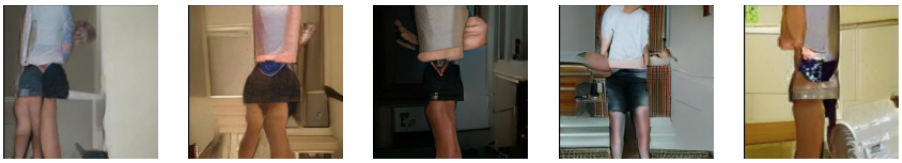

Incorrect

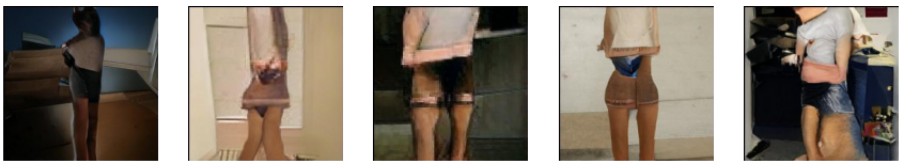

Correct

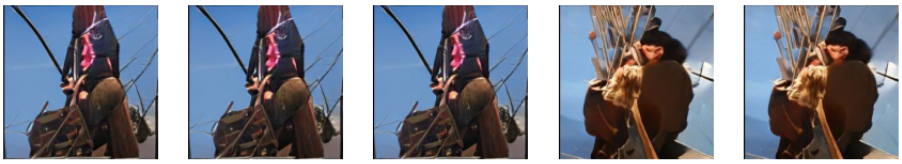

Incorrect

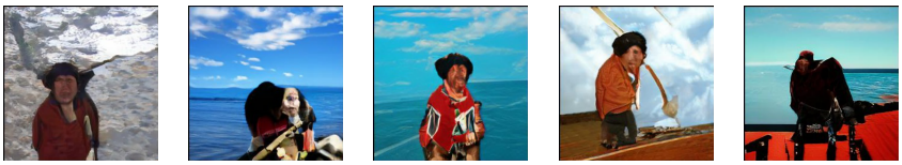

Correct

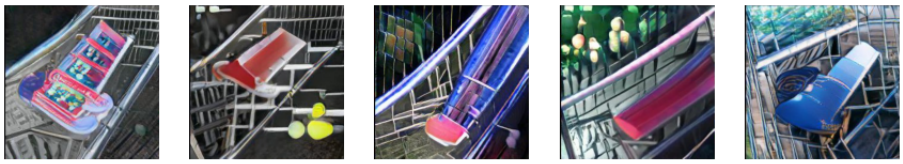

Incorrect

Correct

Incorrect

Bibliography

[1] T. Salimans, I. Goodfellow, W. Zaremba, V. Cheung, A. Radford, and X. Chen. *Improved techniques for training gans.* In NIPS, 2016.

[2] C. Szegedy, V. Vanhoucke, S. Ioffe, J. Shlens, Z. Wojna. *Rethinking the inception architecture for computer vision.* arXiv preprint arXiv: 1512.00567, 2015.

[3] S. Barratt, R. Sharma. *A note on the Inception Score.* arXiv preprint arXiv: 1801.01973, 2018.

[4] M. Heusel, H. Ramsauer, T. Unterthiner, B. Nessler, S. Hochreiter. *GANs trained by a two time-scale update rule converge to a local Nash equilibrium.* In NIPS, 2017.

[5] R. Storn, K. Price. *Differential Evolution – A Simple and Efficient Heuristic for global Optimization over Continuous Spaces.* Springer, 1997.

[6] T. Karras, S. Laine, T. Aila. *A style-based generator architecture for generative adversarial networks.* In CVPR, 2019.

[7] I. Goodfellow et al. *Generative Adversarial Nets* 2014. `https://arxiv.org/pdf/1406.2661.pdf`

[8] M. Brundage, S. Avin, J. Clark et al. *The Malicious Use of Artificial Intelligence: Forecasting, Prevention, and Mitigation.* arXiv preprint arXiv: 1802.07228, 2018.

[9] OpenAI CLIP https://arxiv.org/pdf/2103.00020.pdf

[10] https://www.cs.toronto.edu/ kriz/cifar.html

[11] https://www.image-net.org/

[12] A. Radford, J. W. Kim, C. Hallacy, A. Ramesh, G. Goh, S. Agarwal, G. Sastry, A. Askell, P. Mishkin, J. Clark et al. *Learning transferable visual models from natural language supervision.* In CVPR, 2019.

[13] https://openai.com/blog/clip/

[14] https://habr.com/en/post/537334/

[15] https://github.com/vrakesh/CIFAR-10-Classifier

[16] https://pytorch.org/hub/pytorch_vision_resnet

[17] https://devopedia.org/imagenet

[18] https://machinelearningmastery.com/what-are-generative-adversarial-networks-gan